Journal of Experimental Botany, Vol. 72, No. 6 pp. 2231–2241, 2021
doi:10.1093/jxb/eraa535 Advance Access Publication 14 November 2020

RESEARCH PAPER

Mechanisms underlying iron deficiency-induced resistance against pathogens with different lifestyles

Pauline L. Trapet*, Eline H. Verbon*, Renda R. Bosma, Kirsten Voordendag, Johan A. Van Pelt and Corné M.J. Pieterse†

Plant-Microbe Interactions, Department of Biology, Science4Life, Utrecht University, Padualaan 8, 3584 CH Utrecht, The Netherlands

* These authors contributed equally to this work.
† Correspondence: C.M.J.Pieterse@uu.nl

Received 17 June 2020; Editorial decision 2 November 2020; Accepted 10 November 2020

Editor: Janneke Balk, John Innes Centre, UK

Abstract

Iron (Fe) is a poorly available mineral nutrient which affects the outcome of many cross-kingdom interactions. In *Arabidopsis thaliana*, Fe starvation limits infection by necrotrophic pathogens. Here, we report that Fe deficiency also reduces disease caused by the hemi-biotrophic bacterium *Pseudomonas syringae* and the biotrophic oomycete *Hyaloperonospora arabidopsidis*, indicating that Fe deficiency-induced resistance is effective against pathogens with different lifestyles. Furthermore, we show that Fe deficiency-induced resistance is not caused by withholding Fe from the pathogen but is a plant-mediated defense response that requires activity of ethylene and salicylic acid. Because rhizobacteria-induced systemic resistance (ISR) is associated with a transient up-regulation of the Fe deficiency response, we tested whether Fe deficiency-induced resistance and ISR are similarly regulated. However, Fe deficiency-induced resistance functions independently of the ISR regulators MYB72 and BGLU42, indicating that both types of induced resistance are regulated in a different manner. Mutants *opt3* and *frd1*, which display misregulated Fe homeostasis under Fe-sufficient conditions, show disease resistance levels comparable with those of Fe-starved wild-type plants. Our results suggest that disturbance of Fe homeostasis, through Fe starvation stress or other non-homeostatic conditions, is sufficient to prime the plant immune system for enhanced defense.

Keywords: *Arabidopsis thaliana*, *Botrytis cinerea*, defense priming, *Hyaloperonospora arabidopsidis*, induced resistance, iron homeostasis, plant immunity, *Pseudomonas syringae*.

Introduction

Iron (Fe) functions as an enzyme cofactor in several important cellular processes, such as respiration, DNA synthesis, hormone production, and chlorophyll biosynthesis. Fe is, therefore, an essential nutrient for nearly all living organisms (Darbani *et al.*, 2013; Balk and Schaedler, 2014). As the bioavailability of Fe in soil is generally low (Guerinot and Ying, 1994), plants have developed sophisticated mechanisms to ensure sufficient Fe uptake. Non-grass plant species, such as *Arabidopsis thaliana* (Arabidopsis), make use of an Fe uptake strategy called Strategy I (Römheld, 1987). This Fe uptake strategy is

Abbreviations: BABA, β-aminobutyric acid; cfu, colony-forming units; ET, ethylene; ISR, induced systemic resistance; JA, jasmonic acid; MeJA, methyl jasmonic acid; qRT–PCR, quantitative reverse transcription–PCR; SA, salicylic acid; SAR, systemic acquired resistance.

based on the reduction of ferric Fe (Fe^{3+}) to ferrous Fe (Fe^{2+}), which can then be taken up by the roots via specific plant transporters. A major regulator of Strategy I in Arabidopsis is the transcription factor FER-LIKE IRON DEFICIENCY TRANSCRIPTION FACTOR (FIT). When plants experience Fe deficiency, FIT activates, among a large set of other genes, *FERRIC REDUCTASE OXIDASE2* (*FRO2*), *IRON REGULATED TRANSPORTER1* (*IRT1*), and the transcription factor gene *MYB72* (Colangelo and Guerinot, 2004). FRO2 reduces soilborne Fe^{3+} to Fe^{2+} (Robinson *et al.*, 1999), which is subsequently taken up in the root interior through the Fe transporter IRT1 (Vert *et al.*, 2002).

Roots of Fe-deprived Strategy I plants secrete protons via the H^+-ATPase pump AHA2 to acidify the rhizosphere, thereby increasing Fe solubility in the soil environment (Santi and Schmidt, 2009). In addition, roots of Fe-starved plants produce and secrete Fe-mobilizing phenolic compounds called coumarins in the rhizosphere (Tsai and Schmidt, 2017). The root-specific transcription factor MYB72 is an important regulator of the coumarin biosynthesis pathway (Zamioudis *et al.*, 2014; Stringlis *et al.*, 2018*b*), in which FERULOYL-COA 6'-HYDROXYLASE1 (F6'H1) is a key enzyme (Schmid *et al.*, 2014; Tsai and Schmidt, 2017). Downstream of MYB72, activity of the glycoside hydrolase β-GLUCOSIDASE42 (BGLU42) converts glycosylated coumarins into their aglycone counterparts, which is required for the secretion of the coumarins into the rhizosphere (Zamioudis *et al.*, 2014; Stringlis *et al.*, 2018*b*). The secretion of protons and Fe-chelating coumarins into the soil environment results in Fe solubilization and increased effectivity of FRO2 (Santi and Schmidt, 2009; Fourcroy *et al.*, 2014). Upon IRT1-mediated uptake of Fe by the roots, different Fe transporters, such as YELLOW STRIPE-LIKE (YSL) family members and NRAMPs, take care of the proper distribution of Fe throughout the plant (Kobayashi *et al.*, 2019). As an excess of Fe can cause major damage to cells through the production of hydroxyl radicals (Fenton, 1894), various organic molecules, such as citrate, phenolics, and nicotianamine, act as chaperones during Fe transport to prevent toxicity. Ferritins (FERs), nicotianamine, and phytates are involved in buffering Fe once it is stored in the vacuole, mitochondria, and chloroplasts (Darbani *et al.*, 2013; Kobayashi *et al.*, 2019). Once sufficient Fe has been transported to the shoot, the demand for Fe in the shoot decreases and the uptake of Fe by the roots becomes down-regulated (Connorton *et al.*, 2017). The phloem-specific Fe transporter OLIGOPEPTIDE TRANSPORTER 3 (OPT3) is involved in shoot to root signaling of the leaf Fe status to finely regulate Fe homeostasis throughout the plant (Mendoza-Cózatl *et al.*, 2014; Zhai *et al.*, 2014; García *et al.*, 2018; Khan *et al.*, 2018). Fe availability affects not only plant nutrient status, but also plant susceptibility to disease (Aznar *et al.*, 2015*a*; Verbon *et al.*, 2017). For example, the Arabidopsis defense response to the pathogenic bacterium *Dickeya dadantii* requires sufficient Fe content in the plant, as it involves the release of Fe from the vacuole to develop an oxidative burst that can limit pathogen growth (Segond *et al.*, 2009). In response to pathogen infection, the plant increases the expression of *FERRITIN1* (*FER1*), which encodes an Fe storage protein, probably to protect the as yet uninfected plant tissues from the Fe-mediated oxidative stress (Dellagi *et al.*, 2005; Aznar *et al.*, 2015*b*). The opposite strategy, in which plants do not expose pathogens to an excess of Fe, but rather withhold Fe from the pathogen, is also employed. For example, in response to infection by *Pectobacterium carotovorum* subsp. *carotovorum*, Arabidopsis withholds Fe from the pathogen by enhancing the sequestration of Fe in the apoplast, thereby decreasing pathogen virulence (Hsiao *et al.*, 2017). In the interaction between Arabidopsis and *Pseudomonas syringae* pv. *tomato*, activation of the plant immune system was shown to suppress an Fe acquisition pathway in the pathogen, thereby hampering pathogen virulence (Nobori *et al.*, 2018). In addition to Fe withholding, enhanced pathogen resistance of Fe-deficient plants can in some cases be due to the Fe deficiency-induced secretion of antimicrobial molecules by the plants. An example is the above-described Fe deficiency-induced secretion of coumarins that in addition to their Fe mobilizing activity also possess antimicrobial properties (Beyer *et al.*, 2019; Stringlis *et al.*, 2019). Finally, Fe deficiency has been suggested to induce resistance to necrotrophic pathogens by enhancing the plant's immune response, although the underlying mechanisms are largely unknown (Kieu *et al.*, 2012; Koen *et al.*, 2014).

Interestingly, the Fe deficiency response in roots of Fe-sufficient plants is also transiently activated in response to colonization by beneficial rhizosphere-inhabiting rhizobacteria and fungi that promote plant growth and confer an induced systemic resistance (ISR) that is typically effective against different types of pathogens (Segarra *et al.*, 2009; Pieterse *et al.*, 2014; Martínez-Medina *et al.*, 2017; Romera *et al.*, 2019; Verbon *et al.*, 2019). This phenomenon is particularly well studied in the interaction between Arabidopsis and the beneficial rhizobacterium *Pseudomonas simiae* WCS417 (Pieterse *et al.*, 2014, 2020). *MYB72* and *BGLU42* are among the Fe deficiency response genes that are also activated upon colonization of the roots by WCS417 bacteria (Van der Ent *et al.*, 2008; Zamioudis *et al.*, 2014; Stringlis *et al.*, 2018*a*). As described above, MYB72 and BGLU42 are involved in the secretion of Fe-chelating coumarins that increase Fe^{3+} availability in the soil environment (Schmid *et al.*, 2014; Fourcroy *et al.*, 2016; Tsai and Schmidt, 2017; Stringlis *et al.*, 2019). Indeed, colonization of the roots by WCS417 improves Fe nutrition in Arabidopsis (Verbon *et al.*, 2019). Interestingly, mutant *myb72* and *bglu42* plants are incapable of mounting WCS417-ISR, indicating that both MYB72 and BGLU42 are also required for the onset of ISR (Van der Ent *et al.*, 2008; Segarra *et al.*, 2009; Zamioudis *et al.*, 2014). Overexpression of BGLU42 in *oxBGLU42* plants results in constitutively enhanced disease resistance against different pathogens (Zamioudis *et al.*, 2014), pinpointing the MYB72/BGLU42 module as an intrinsic component of both the Fe deficiency and the ISR signaling pathway (Stassen *et al.*,

2020). WCS417-ISR is characterized by a 'sensitization' of the plant's immune system resulting in enhanced activation of defenses only after pathogen or insect attack (Pieterse *et al.*, 2014). This phenomenon is known as defense priming and provides the plant with a cost-effective mechanism of protection against pathogens and pests (Martinez-Medina *et al.*, 2016). In the case of WCS417-ISR, the defense hormones jasmonic acid (JA) and ethylene (ET) play important regulatory roles (Pieterse *et al.*, 1998).

Plant defense hormones ET, JA, and salicylic acid (SA) act as cellular signaling molecules in the regulation of the immune processes that are activated in response to microbial pathogens, insect herbivores, and beneficial microbes. The hormone signaling pathways are interconnected in a complex network to allow plants to rapidly adapt to their biotic and abiotic environment and to utilize limited resources in a cost-efficient manner (Pieterse *et al.*, 2012). In Arabidopsis, SA is required for an adequate defense response to (hemi)biotrophic pathogens that need living host cells to feed on, while JA and ET are involved in the defense response against necrotrophic pathogens that first kill host cells, after which they feed on the contents. Besides activating local defense responses, these plant defense hormones act in systemic immune responses, such as rhizobacteria-mediated ISR (Pieterse *et al.*, 1998; Ton *et al.*, 2001), pathogen-induced systemic acquired resistance (SAR) (Durrant and Dong, 2004; Vlot *et al.*, 2008), and herbivory- or wound-induced resistance (Howe and Jander, 2008; Wu and Baldwin, 2010). SA and ET are also positive regulators of the Fe uptake response, whereas JA is a negative regulator (Hindt and Guerinot, 2012; Brumbarova *et al.*, 2015; Shen *et al.*, 2016; Romera *et al.*, 2019). The dual role of these hormones in Fe nutrition and immunity, combined with the observation that WCS417-ISR is controlled by signaling components that also play a role in the Fe deficiency response (Zamioudis *et al.*, 2015), suggests an intrinsic interplay between the maintenance of Fe homeostasis and plant immunity.

In this study, we investigated the biological mechanisms underlying Fe deficiency-induced resistance and its relationship to WCS417-ISR. We found that, like WCS417-ISR, Fe deficiency-induced resistance is a plant-mediated defense response that is effective against pathogens with different lifestyles, but their signaling pathways are, at least partially, regulated differently. We provide evidence that disturbance of Fe homeostasis is sufficient for the onset of Fe deficiency-induced resistance.

Materials and methods

Plant material and growth conditions

Wild-type *A. thaliana* accession Columbia-0 (Col-0), and the mutants *myb72-2* (Van der Ent *et al.*, 2008), *bglu42* (Zamioudis *et al.*, 2014), *frd1-1* (Robinson *et al.*, 1999), *opt3-2* (Stacey *et al.*, 2008), *ein2-1* (Guzman and Ecker, 1990), and *sid2-1* (Wildermuth *et al.*, 2001), and the *BGLU42*-overexpressing line *oxBGLU42* (Zamioudis *et al.*, 2014), all in the Col-0 background, were grown in hydroponic culture as described previously (Trapet *et al.*, 2016), with minor modifications. Briefly, vapor-phase sterilized seeds were stratified at 4 °C in half-strength modified Hoagland medium supplemented with 0.2% agar, with full-strength standard Hoagland medium (referred to as +Fe medium) containing 0.2 mM $Ca(NO_3)_2$, 0.5 mM KNO_3, 0.25 mM KH_2PO_4, 0.2 mM $MgSO_4$, 70 μM H_3BO_3, 14 μM $MnCl_2$, 1.0 μM $ZnSO_4$, 0.5 μM $CuSO_4$, 10 μM NaCl, 0.2 μM Na_2MoO_4, and 50 μM FeNaEDTA. After 4 d, seeds were sown on seed holders filled with 10-fold diluted +Fe medium supplemented with 0.65% agar, and placed on top of hydroponic bins (Araponics, Liège, Belgium). The bins were filled with +Fe medium and placed in short-day growth conditions (21–22 °C, 14 h night, 10 h day, light intensity 100 μmol m^{-2} s^{-1}). A transparent lid was put on the bins for the first 10 d to maintain the high humidity necessary for proper seed germination. The hydroponic growth medium was renewed weekly from 2 weeks onwards. After 3 weeks, the plants were rearranged from a high-density set-up (35 plants per bin) to a low-density set-up (18 plants per bin) in which the liquid medium was aerated. The Fe deficiency response mutant *frd1-1*, which carries a mutation in the *FRO2* gene (Robinson *et al.*, 1999), was cultivated in +Fe medium supplemented to a final concentration of 300 μM FeNaEDTA, as it is not viable in +Fe medium containing 50 μM FeNaEDTA. The Fe deficiency treatment was performed after 25–32 d of growth on Fe-sufficient medium, dependent on the experiment and as specified below. To this end, the liquid medium in the hydroponic bins was replaced with either +Fe medium (50 μM Fe, or 300 μM Fe for *frd1-1*) or medium without added FeNaEDTA (referred to as –Fe medium). To limit transfer of adhering Fe from the +Fe medium to the –Fe medium, roots were rinsed in –Fe medium before transfer to either fresh –Fe or +Fe medium.

Pathogen bioassays

Cultivation of the pathogens, preparation of the pathogen inocula, inoculation of the plants, and measurements of disease severity were carried out as described previously (Van Wees *et al.*, 2013), with some minor modifications. Pathogen inoculation was performed 3 d after the final transfer of the plants to +Fe or –Fe medium.

Botrytis cinerea strain B05.10 (Van Kan *et al.*, 2017) was cultivated on half-strength potato dextrose agar plates for 10 d at 22 °C (16 h night, 8 h day). Spores were harvested in half-strength potato dextrose broth, filtered through gauze, and resuspended to an inoculum containing 5×10^5 spores ml^{-1}. Hydroponically grown plants were inoculated when they were 5 weeks old by applying a 5 μl droplet of the *B. cinerea* inoculum onto five mature leaves per plant. The bins containing the inoculated plants were kept in closed trays to ensure high humidity for optimal pathogen development. Inoculated leaves were harvested, and pictures were taken at 3 d post-inoculation. Lesion area was measured using the publicly available image analysis program ImageJ (version 1.51n).

Pseudomonas syringae pv. *tomato* DC3000 (Kunkel *et al.*, 1993) was cultivated overnight on King's medium B agar plates (King *et al.*, 1954) at 28 °C. Subsequently, bacteria were collected in 10 mM $MgSO_4$ and washed twice by 5 min centrifugation at 5000 *g*. The bacteria were then resuspended to a density of 2.5×10^7 colony-forming units (cfu) ml^{-1} (OD_{660}=0.025) in 10 mM $MgSO_4$ amended with 0.02% (v/v) Silwet L-77 (Van Meeuwen Chemicals, Weesp, The Netherlands). Five-week-old plants were inoculated by dipping their rosette into the bacterial suspension for 3 s. The bins containing the inoculated plants were kept in closed trays to ensure high humidity. After 3 d, bacterial growth was determined in two leaf discs harvested from two different leaves per infected plant. The two leaf discs per plant were pooled and lysed using beads in 500 μl of 10 mM $MgSO_4$. Serial dilutions were plated on King's medium B agar containing 25 mg ml^{-1} rifampicin to determine *in planta* bacterial growth.

Hyaloperonospora arabidopsidis isolate Noco2 (Lapin *et al.*, 2012) was maintained on susceptible Arabidopsis mutant *eds1* plants as described (Van Damme *et al.*, 2009). Spores were obtained from these plants by washing infected seedlings in demi water. The spore suspension was filtered through Miracloth and the final concentration was adjusted to 1×10^5 spores ml^{-1}. Four-week-old plants were sprayed with the *H. arabidopsidis* inoculum and kept in closed trays to ensure high humidity. To facilitate development of the *H. arabidopsidis* infection, the trays were placed in growth conditions optimal for *H. arabidopsidis* development (16 °C; 9 h day, 15 h night). Two weeks after inoculation, plants were weighed and collected in a 50 ml conical tube containing 3 ml of demi water. After vigorous shaking, the number of *H. arabidopsidis* spores in the suspension was estimated using a Bürker counting chamber. In addition to spore counting, *H. arabidopsidis* disease severity was assessed by visualizing hyphal growth using trypan blue staining. Two weeks after inoculation, six leaves were harvested from three plants per treatment. The leaves were boiled for 2–10 min in 1 ml of trypan blue solution [1:1:1:1 lactic acid:glycerol:phenol:water and 25% (w/v) trypan blue]. After incubating for 1 h at room temperature, the solution was replaced by chloral hydrate for destaining overnight. Hyphal growth in the leaves, visible as strong blue coloration, was inspected using light microscopy.

Hormone treatment

Hormonal treatments were performed as described previously (Van Wees *et al.*, 2013) on 4-week-old plants, 3 d after the final transfer to either +Fe or –Fe medium. In brief, 4-week-old plants were treated with methyl JA (MeJA) by dipping the leaves for 4 s into a solution containing 0.015% (v/v) Silwet L-77, 0.1% EtOH, and 100 µM MeJA (Serva, Brunschwig Chemie, Basel, Switzerland). Mock treatments were dipped into a solution containing 0.0015% (v/v) Silwet L-77 and 0.1% EtOH. Plants were then placed back in the hydroponic bins. Shoots were harvested and immediately frozen in liquid nitrogen at 6, 12, and 24 h after treatment. Tissues were stored at –80 °C until RNA isolation.

RNA isolation and RT–qPCR

RNA was isolated from tissue samples using the protocol described previously (Oñate-Sánchez and Vicente-Carbajosa, 2008). DNase I (Thermo Fisher Scientific, Waltham, MA, USA) treatment was applied to RNA samples according to the manufacturer's instructions. RNA samples were reverse transcribed to cDNA using RevertAid H Minus Reverse Transcriptase (Thermo Fisher Scientific), according to the manufacturer's instructions. Quantitative reverse transcription–PCR (qRT–PCR) was performed on cDNA using Power SYBR green PCR master mix (Applied Biosystems, Waltham, MA, USA) with gene-specific primers. The cycle threshold (Ct) was determined using the ViiA 7 Real-Time PCR system (Applied Biosystems). Gene expression data were normalized to the gene *PP2AA3* (*At1g13320*) (Czechowski *et al.*, 2005). Evidence of invariant expression of *PP2AA3* under the conditions used is provided in Supplementary Fig. S1. Relative quantification of specific mRNA levels was performed using the comparative $2^{-\Delta\Delta Ct}$ method (Schmittgen and Livak, 2008). The ΔΔCt values were used for statistical analyses, and the relative gene expression ($2^{-\Delta Ct}$) was plotted. The following primers were used: *FIT*-forward, 5'-AAC CTA AGC TCT CCT TCT CC-3'; *FIT*-reverse, 5'-GCA AGT TTA AGC TCT GTT CG-3'; *VSP2*-forward, 5'-ATG CCA AAG GAC TTG CCC TA-3'; *VSP2*-reverse, 5'-CGG GTC GGT CTT CTC TGT TC-3'; *PP2AA3*-forward, 5'-TAA CGT GGC CAA AAT GAT GC-3'; and *PP2AA3*-reverse, 5'-GTT CTC CAC AAC CGC TTG GT-3'. Arabidopsis gene identifier numbers are: *FIT* (At2g28160); *VSP2* (At5g24770); and *PP2AA3* (At1g13320).

Fe content measurement

Four-week-old Col-0 and *opt3-2* plants were transferred to +Fe or –Fe medium. Shoots were harvested for Fe content measurement at 7 d after transfer. The samples were dried and mineralized as described previously (Verbon *et al.*, 2019). Fe content was subsequently measured by inductively coupled plasma-atomic emission spectroscopy (iCAP 6000 Series, Thermo Fisher Scientific).

Results

Fe deficiency confers enhanced resistance against pathogens with different lifestyles

In Arabidopsis, Fe deficiency has been shown to enhance resistance to necrotrophic leaf pathogens (Kieu *et al.*, 2012; Trapet *et al.*, 2016). To study the spectrum of effectiveness of this Fe deficiency-induced resistance, we first established a hydroponic experimental set-up with Fe-sufficient and Fe-deficient plants. In this hydroponic system, Fe-sufficient wild-type Arabidopsis Col-0 plants were first grown on Fe-sufficient liquid Hoagland medium, after which they were transferred to either Fe-sufficient or Fe-deficient medium (Fig. 1A). Plants grown in Fe-deficient medium developed typical signs of Fe deficiency: reduction of plant growth (Fig. 1B); a chlorotic phenotype (Fig. 1C); reduction in chlorophyll content (Fig. 1D); and activation of the Fe deficiency response master regulatory gene *FIT* (Fig. 1E).

To test the effect of Fe deficiency on disease susceptibility to pathogens with different lifestyles, leaves of Fe-sufficient and Fe-deficient Col-0 plants were inoculated with the necrotrophic fungus *B. cinerea*, the hemi-biotrophic bacterium *P. syringae* pv. *tomato* DC3000, or the obligate biotrophic oomycete *H. arabidopsidis*, according to the inoculation scheme depicted in Fig. 2A. Fe-starved Col-0 plants showed significantly fewer disease symptoms than Fe-sufficient Col-0 plants after infection with all three pathogens (Fig. 2B–D). Thus, Fe deficiency confers enhanced resistance to pathogens with diverse lifestyles.

Previously, we demonstrated that overexpression of the Fe deficiency-responsive gene *BGLU42* in *oxBGLU42* plants grown in soil with sufficient Fe is associated with enhanced resistance against *B. cinerea*, *P. syringae* pv. *tomato* DC3000, and *H. arabidopsidis* (Zamioudis *et al.*, 2014). To investigate to what extent this *oxBGLU42*-mediated disease resistance reflects Fe deficiency-induced resistance, we monitored disease severity levels against *B. cinerea, P. syringae* pv. *tomato* DC3000, and *H. arabidopsidis* in Col-0 and *oxBGLU42* plants grown hydroponically on Fe-sufficient and Fe-deficient medium. Figure 2B–D shows that when Col-0 and *oxBGLU42* plants were grown on Fe-sufficient medium, *oxBGLU42* plants displayed an enhanced level of resistance against all three pathogens, confirming previous findings with Fe-sufficient soil-grown plants (Zamioudis *et al.*, 2014). The level of disease severity in Fe-sufficient *oxBGLU42* plants was reduced to a similar level

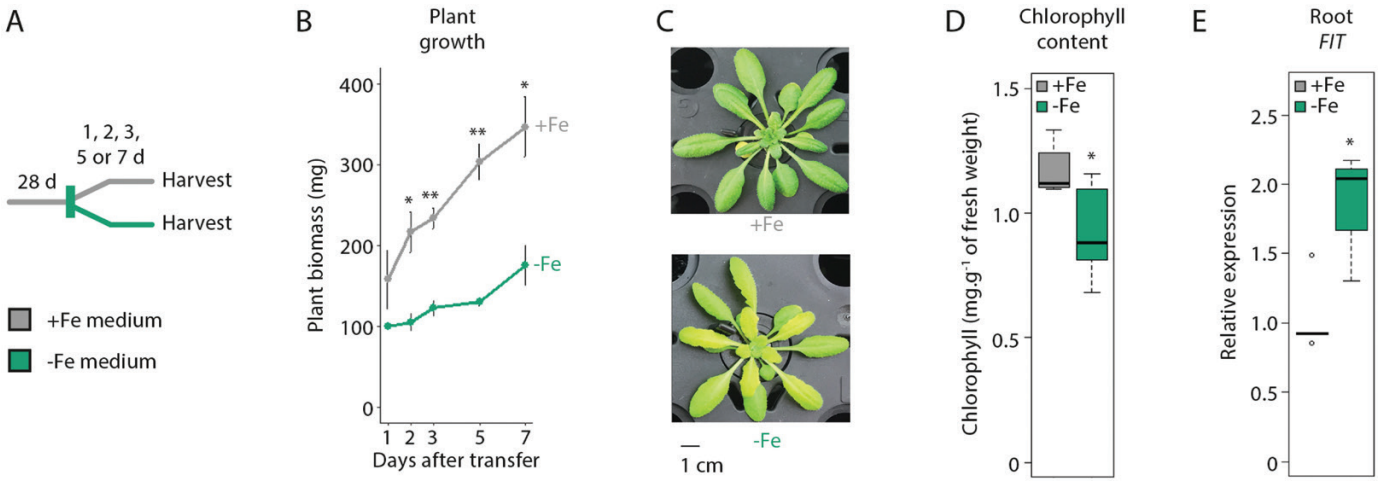

Fig. 1. Effect of Fe deficiency on plant growth and Fe homeostasis in hydroponically grown Arabidopsis plants. (A) Schematic representation of the experimental design using a hydroponic Arabidopsis culturing system. Four-week-old plants grown with their roots in modified Hoagland medium containing Fe (+Fe; gray) were transferred to fresh +Fe medium or to medium lacking Fe (–Fe; green). Plant roots and shoots were harvested for analyses at the indicated number of days after transfer. (B) Biomass of wild-type Col-0 plants at 1, 2, 3, 5, and 7 d after transfer. Per time point, asterisks indicate a significant difference between the +Fe and –Fe treatment (Student's *t*-test; **P*<0.05, ***P*<0.005; *n*=3). Representative pictures (C), chlorophyll content (D), and qRT–PCR analysis of *FIT* gene expression in the root (E) at 7 d after transfer. Gene expression levels were normalized to that of the constitutively expressed gene *PP2AA3* (At1g13320). Fold changes in gene expression levels relative to the average of the control plants are plotted. Error bars represent the SEM. Asterisks indicate a significant difference between the +Fe and –Fe treatment (Student's *t*-test; **P*<0.05, ***P*<0.005, *n*=3–6).

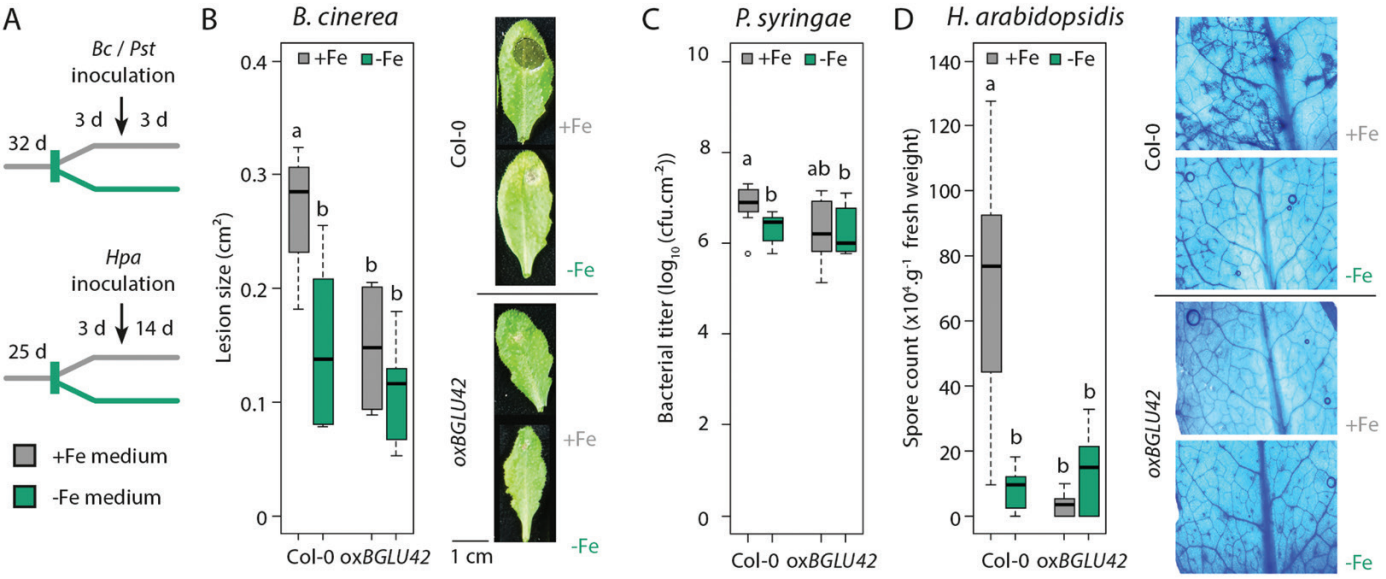

Fig. 2. Effect of Fe deficiency on disease resistance against pathogens with different lifestyles. (A) Schematic representation of the experimental design using a hydroponic Arabidopsis culturing system. Plants were first grown with their roots in liquid medium containing Fe (+Fe) for the indicated number of days, after which they were transferred to a fresh +Fe medium or a medium without Fe (–Fe) 3 d before pathogen inoculation. Inoculations with *Botrytis cinerea* and *Pseudomonas syringae* pv. *tomato* DC3000 were performed on 35-day-old plants, and inoculation with *Hyaloperonospora arabidopsidis* on 28-day-old plants. Disease severity was evaluated 3 d or 14 d later, as indicated. (B) Level of disease severity of Fe-sufficient (+Fe) and Fe-deficient (–Fe) Col-0 and ox*BGLU42* plants after inoculation with *B. cinerea.* Values represent the mean lesion area per leaf calculated from five inoculated leaves per plant. Pictures show representative disease symptoms. (C) Disease severity after inoculation with *P. syringae* pv. *tomato* DC3000. Values represent the number of colony-forming units (cfu) per cm^2 leaf. (D) Disease severity after inoculation with *H. arabidopsidis.* Values represent the number of spores per gram of leaf fresh weight. Pictures show trypan blue staining of *H. arabidopsidis* colonization of the leaves. Different letters indicate statistically significant differences (two-way ANOVA/Tukey HSD test, *P*<0.05, *n*=4–8).

to that observed in Fe-starved Col-0 plants and was not reduced further in Fe-starved *oxBGLU42* plants. These results indicate that *oxBGLU42*-mediated enhanced disease resistance against pathogens with different lifestyles is a phenocopy of the broad-spectrum disease resistance observed in Fe-starved wild-type Col-0 plants.

Fe deficiency-induced resistance is associated with defense priming

The plant hormones ET and SA are implicated in both the Fe deficiency response and plant immunity (Broekgaarden *et al.*, 2015; Lucena *et al.*, 2015; Shen *et al.*, 2016; García *et al.*, 2018; Zhang and Li, 2019). Here, we tested whether ET and SA play a role in the development of Fe deficiency-induced resistance against the necrotroph *B. cinerea*. To this end, we made use of the ET signaling mutant *ein2-1* and the SA biosynthesis mutant *sid2-1*, both of which have been reported to be affected in induced defenses against *B. cinerea* (Thomma *et al.*, 1999; Segarra *et al.*, 2013). We found that Fe starvation significantly induced resistance against *B. cinerea* in wild-type Col-0, but not in the hormone mutants tested (Fig. 3A). The observation that conditions of Fe starvation did not reduce pathogen virulence in either *ein2-1* or *sid2-1* suggests that in wild-type Col-0 plants the observed enhanced level of resistance is mediated by Fe deficiency-induced plant defense responses, rather than by direct effects of Fe limitation on pathogen virulence. This was further substantiated by our finding that *sid2-1* was also impaired in Fe deficiency-induced resistance against *H. arabidopsidis* (Fig. 3B). Mutant *sid2-1* plants showed significantly enhanced susceptibility to downy mildew infection when exposed to Fe deficiency (Fig. 3B), while Fe-starved Col-0 plants showed reduced colonization of the pathogen (Fig. 3B right panel) and produced fewer spores (Fig. 3B left panel), albeit not statistically significant in this experiment.

Many types of broad-spectrum induced resistance are often (partly) based on defense priming, a defensive state in which plants do not show direct activation of immune responses following stimulation, but are conditioned to react faster and/or more strongly to subsequent pathogen or insect attack (Martinez-Medina *et al.*, 2016). Because Fe deficiency-induced resistance is effective against pathogens with different lifestyles, we tested whether defense priming plays a role in this phenomenon. To this end, we mimicked necrotrophic pathogen infection by dipping the leaves of hydroponically grown Col-0 plants, growing on either Fe-sufficient or Fe-deficient medium, in MeJA, after which we monitored the expression of the JA-responsive marker gene *VSP2* over time (Fig. 3C). In mock-treated plants, the expression profile of the *VSP2* marker gene was similar in both Fe-sufficient and Fe-deficient plants,

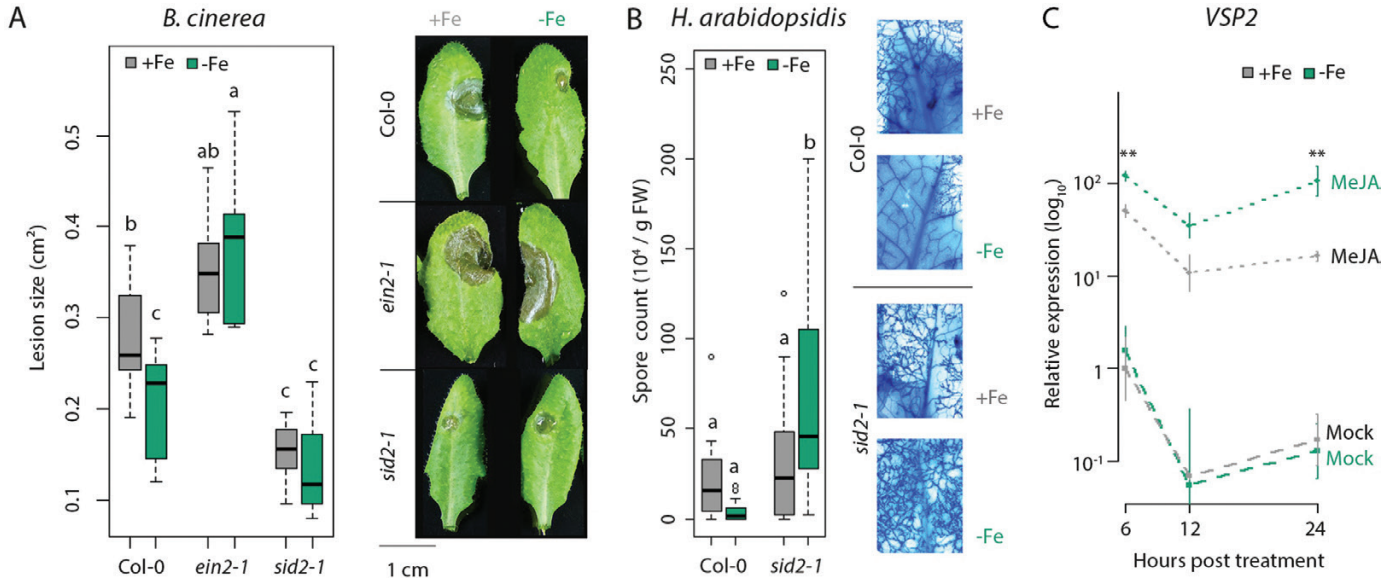

Fig. 3. Fe deficiency-induced resistance in hormone-impaired Arabidopsis mutants *ein2-1* and *sid2-1*, and effect on defense priming. (A) Disease severity in Col-0, *ein2-1*, and *sid2-1* plants grown with their roots in medium containing Fe (+Fe, gray) or medium without Fe (–Fe, green), at 3 d after inoculation with *Botrytis cinerea*. The disease ratings are expressed as the mean lesion area from five inoculated leaves per plant (n=5–13). Representative pictures of the inoculated leaves are shown. (B) Disease severity in +Fe and –Fe Col-0 and *sid2-1* plants at 14 d after inoculation with *Hyaloperonospora arabidopsidis*. Disease severity is expressed as the number of spores per gram of fresh weight. Representative pictures of hyphal growth, visualized by trypan blue staining, are shown (all taken with the same magnification). Different letters indicate statistically significant differences (two-way ANOVA/Tukey HSD method, P<0.05, n=5–20). (C) qRT–PCR analysis of *VSP2* gene expression in the shoots of 4-week-old Fe-sufficient (+Fe) and Fe-deficient (–Fe) Col-0 plants treated with methyl jasmonate (MeJA) or with a mock treatment (Mock). Gene expression levels were normalized to that of the constitutively expressed gene *PP2AA3* (At1g13320). Log_{10} of the fold changes in gene expression levels relative to the average of the control plants are plotted. Error bars represent the SEM. Per time point and per hormonal treatment (mock or MeJA), asterisks indicate a significant difference between the +Fe and –Fe treatment (Student's t-test; *P<0.05, **P<0.01, n=4).

indicating that *VSP2* was not directly activated in response to conditions of Fe deficiency. Exogenous application of MeJA to the leaves induced the expression of *VSP2* in both Fe-sufficient and Fe-deficient Col-0 plants. At all time points tested, MeJA-induced *VSP2* transcription was higher in Fe-deficient plants. These results indicate that Fe deficiency-induced resistance is associated with defense priming.

Fe deficiency-induced resistance does not require the ISR regulators MYB72 and BGLU42

The transcriptional response of Arabidopsis roots to Fe deprivation or colonization by WCS417 bacteria shows a significant overlap: 20% of the WCS417-induced genes are also activated in response to Fe starvation (Zamioudis *et al.*, 2015). Moreover, Fe deficiency-induced resistance, *oxBGLU42*-mediated resistance, and WCS417-ISR are all effective against *B. cinerea*, *P. syringae* pv. *tomato* DC3000, and *H. arabidopsidis* (Fig. 2) (Pieterse *et al.*, 1996; Van der Ent *et al.*, 2008). Therefore, we hypothesized that these two types of induced resistance may be regulated by the same signaling pathway. To test this, we studied Fe deficiency-induced resistance in mutants *myb72-2* and *bglu42*, which have been shown to be impaired in coumarin secretion and the onset of WCS417-ISR, but have an otherwise intact Fe deficiency response machinery (Van der Ent *et al.*, 2008; Segarra *et al.*, 2009; Zamioudis *et al.*, 2014). Figure 4 shows that *myb72-2* and *bglu42* grown on Fe-sufficient medium displayed a similar level of *B. cinerea* disease severity to wild-type Col-0, confirming previous findings (Van der Ent *et al.*, 2008; Zamioudis *et al.*, 2014). When grown on Fe-deficient medium, both ISR mutants mounted a significant Fe deficiency-induced resistance against *B. cinerea*. These results indicate that, in contrast to WCS417-ISR against *B. cinerea*, Fe deficiency-induced resistance functions independently of the ISR regulators MYB72 and BGLU42.

Fe deficiency-induced resistance is associated with disturbances in Fe homeostasis

Conditions of Fe deficiency induce a disease resistance that is effective against pathogens with diverse lifestyles. We wondered whether this effect on plant immunity is specifically linked to physical Fe shortage or may also be triggered in response to other conditions that affect Fe homeostasis. To test this, we selected two mutants with a disturbed Fe uptake response: the leaf Fe status shoot to root signaling mutant *opt3-2* (Stacey *et al.*, 2008) and the FRO2-deficient mutant *frd1-1* (Robinson *et al.*, 1999). The *opt3-2* mutant is impaired in leaf Fe status shoot to root signaling (Mendoza-Cózatl *et al.*, 2014; Zhai *et al.*, 2014). As a result, it displays a constitutively active Fe deficiency response in the roots, while it overaccumulates Fe in the shoot (Zhai *et al.*, 2014; García *et al.*, 2018). The *frd1-1* mutant lacks FRO2 activity and is thus deficient in taking up Fe from the root environment via Strategy I. As a result, it

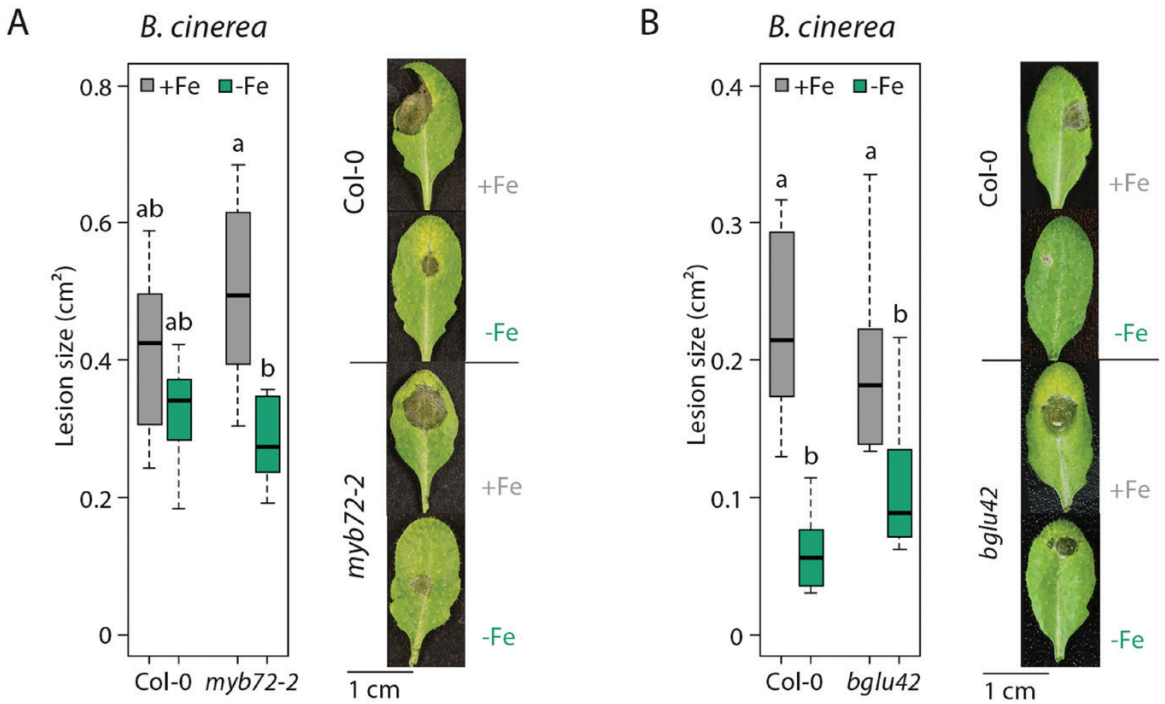

Fig. 4. Fe deficiency-induced resistance in ISR-impaired Arabidopsis mutants *myb72-2* and *bglu42*. Disease severity on Col-0, *myb72-2* (A), and *bglu42* (B) plants grown with their roots in medium containing Fe (+Fe, gray) or medium without Fe (–Fe, green), at 3 d after inoculation with *Botrytis cinerea*. Boxplots show the distribution of the mean lesion area per plant, calculated from the lesion area of five inoculated leaves. Pictures show representative disease symptoms. Different letters indicate statistically significant differences (two-way ANOVA/Tukey HSD method, $P<0.05$, $n=5–12$).

typically has a low Fe content throughout the plant (Yi and Guerinot, 1996; Robinson *et al.*, 1999). Indeed, in our hydroponics set-up, Fe-sufficient *opt3-2* plants displayed higher Fe levels in the shoots compared with wild-type Col-0 plants (Fig. 5A), although this effect was reduced when plants were grown under Fe deficiency. Moreover, the *frd1-1* mutant required Fe supplementation in the Fe- sufficient medium to prevent severe chlorosis. On Fe-sufficient medium, both *opt3-2* and *frd1-1* displayed an enhanced level of resistance against *B. cinerea* in comparison with Fe-sufficient Col-0 plants (Fig. 5B, C). The level of *B. cinerea* resistance in the *opt3-2* and *frd1-1* mutant was similar to that observed in Col-0 growing on Fe-deficient medium (Fig. 5B, C). Growth of *opt3-2* and *frd1-1* on Fe-deficient medium did not change the level of induced resistance against *B. cinerea*. The mutants and Fe-starved Col-0 plants have in common that they all display a disturbed regulation of Fe homeostasis. We therefore hypothesize that a change in Fe homeostasis is sufficient for the onset of Fe deficiency-induced resistance.

Discussion

Maintaining Fe homeostasis is an important determinant of plant performance (Guerinot and Ying, 1994; Balk and Schaedler, 2014; Connorton *et al.*, 2017). Here we investigated the link between the Fe deficiency response and plant immunity. Previously, conditions of Fe deficiency were found to induce resistance against necrotrophic pathogens, such as *D. dadantii* and *B. cinerea* (Kieu *et al.*, 2012). In the present study, we found that Fe-limiting conditions induce a type of disease resistance in Arabidopsis that is also effective against pathogens with a (hemi)biotrophic lifestyle (Fig. 2). The broad-spectrum effectiveness of Fe deficiency-induced resistance resembles that of other types of induced resistance, such as pathogen-induced SAR, rhizobacteria-ISR, and β-aminobutyric acid (BABA)-induced resistance (Durrant and Dong, 2004; Koen *et al.*, 2014; Pieterse *et al.*, 2014). Both rhizobacteria-ISR and BABA-induced resistance have been shown to involve a transient activation of the Fe deficiency response (Koen *et al.*, 2014; Zamioudis *et al.*, 2015; Romera *et al.*, 2019). Overexpression of the ISR regulator BGLU42, which in the Fe deficiency response is responsible for the conversion of glycosylated coumarins into their aglycone counterparts, phenocopied the broad-spectrum disease resistance that was observed in Fe-starved wild-type plants (Fig. 2). Moreover, the defense-related hormones ET and SA, which are involved in both the Fe deficiency response and rhizobacteria-ISR or BABA-induced resistance, respectively (Pieterse *et al.*, 1998; Ton *et al.*, 2005; Lucena *et al.*, 2015; Shen *et al.*, 2016; García *et al.*, 2018), appeared to play a role in Fe deficiency-induced resistance (Fig. 3). However, when we tested the ISR-impaired mutants *myb72-2* and *bglu42* for their capacity to mount Fe

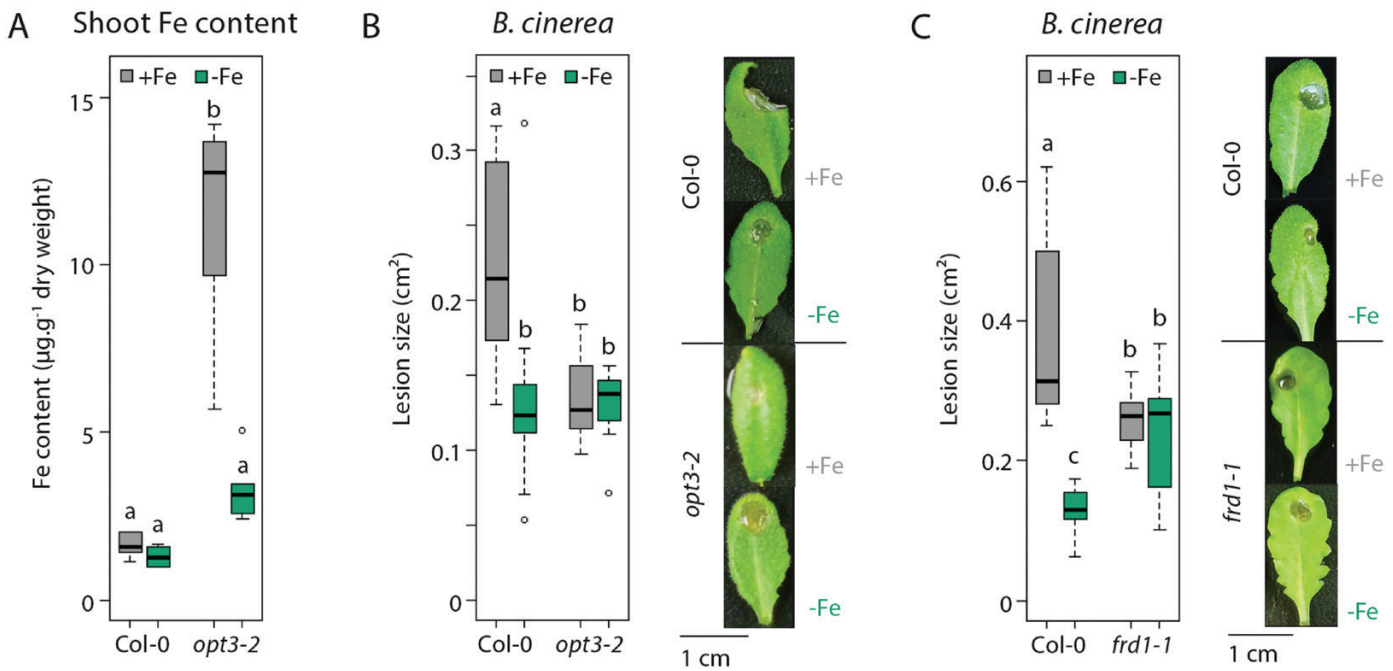

Fig. 5. Fe deficiency-induced resistance in Fe homeostasis-impaired Arabidopsis mutants *opt3-2* and *frd1-1*. (A) Fe content in the shoot of 5-week-old Col-0 and *opt3-2* plants grown for 7 d with their roots in medium containing Fe (+Fe, gray) or medium without Fe (–Fe, green). (B, C) Levels of disease severity in Fe-sufficient (+Fe) and Fe-deficient (–Fe) Col-0, *opt3-2* (B), and *frd1-1* (C) plants, at 3 d after inoculation with *Botrytis cinerea*. The disease ratings are expressed as the mean lesion area per leaf calculated from five inoculated leaves per plant. Different letters indicate statistically significant differences (two-way ANOVA/Tukey HSD method, $P<0.05$, $n=4–5$ for A, 6–17 for B and C).

deficiency-induced resistance against *B. cinerea*, they showed similar levels of resistance to Fe-starved wild-type plants (Fig. 4). We thus concluded that rhizobacteria-ISR and Fe deficiency-induced resistance are regulated, at least partly, via distinct pathways. Previously, it was shown that low Fe availability enhanced the level of rhizobacteria-ISR (Leeman *et al.*, 1996), suggesting that Fe deficiency-induced resistance and rhizobacteria-ISR act additively.

Our observations with mutants *opt3-2* and *frd-1* (Fig. 5) hinted that disturbance of Fe homeostasis *per se* may already be sufficient for the development of enhanced disease resistance. In this scenario, Fe starvation, genetic perturbation of the Fe deficiency response, colonization of the roots by ISR-inducing rhizobacteria, and exogenous application of chemicals, such as BABA, that affect the Fe deficiency response, may all confer different disturbances in Fe homeostasis, which in turn leads to defense priming and enhanced resistance against different types of pathogens. The nature of the primed defense responses that contribute to the enhanced level of disease resistance in Fe-starved plants against the three pathogens tested remains unknown. Fe withholding from the pathogens in Fe-starved plants seems unlikely, because conditions of Fe starvation did not inhibit pathogen development in mutants *ein2-1* and *sid2-1* as compared with Fe-sufficient growth conditions (Fig. 3A, B). Previously, Arabidopsis defenses initiated upon *P. syringae* infection were shown to suppress a cluster of *P. syringae* genes associated with Fe uptake from the host (Nobori *et al.*, 2018), but whether this process is targeted during Fe deficiency-induced resistance remains to be investigated.

Besides Fe, sulfur (S), nitrogen (N), and phosphorus (P) have also been reported to affect plant immunity. S has long been recognized for its fungicidal effect and is widely used to prevent fungal diseases. S fertilization promotes the production of S-containing defense-related metabolites, such as glutathione, phytoalexins, and glucosinolates. Hence, S fertilization leads to S-induced resistance, and S deficiency can impair plant defenses (Bloem *et al.*, 2015). N fertilization, on the contrary, increases rice and wheat sensitivity to blast disease (Ballini *et al.*, 2013), while N starvation can increase the resistance of *Medicago truncatula* against *Aphanomyces euteiches*, potentially through modification of nitric oxide homeostasis (Thalineau *et al.*, 2016, 2018). Phosphate (Pi) starvation results in a plant response that shares features with the activation of the JA signaling pathway and enhances resistance towards herbivores in several plant species (Khan *et al.*, 2016), for example via the accumulation of defense-related secondary metabolites (Luo *et al.*, 2019). Pi deficiency is known to affect Fe distribution in plants (Hirsch *et al.*, 2006), indicating that different nutrient deficiency responses are interconnected. The observation that plant nutrient status modulates the plant immune system and, through excretion of secondary metabolites, can recruit plant-associated microbiota that aid in maintaining nutrient homeostasis (Bakker *et al.*, 2018) highlights the intricate relationship between plant nutrition and the outcome of pathogenic and mutualistic plant–microbe interactions. Future research should therefore be focused on obtaining a detailed understanding of how nutrient deficiencies impact plant–microbe interactions, and how this can contribute to improve plant performance and survival in both natural and agricultural settings.

Supplementary data

The following supplementary data are available at *JXB* online.

Fig. S1. qRT–PCR analysis of transcript levels of the constitutively expressed reference gene *PP2AA3* in roots and shoots of Fe-sufficient (+Fe) and Fe-starved (–Fe) Arabidopsis Col-0 plants grown in hydroponic cultures under the experimental conditions used in this study.

Acknowledgements

We acknowledge Professor Mary Lou Guerinot (Darthmouth College, USA) for providing the *frd1* mutant line. In addition, we thank Gerrit Rouwenhorst and Kim Baremans for technical assistance and Juan Sanchez Gill for critical reading of the manuscript. The authors of this paper are supported by the Netherlands Organization of Scientific Research through ALW Topsector Grant no. 831.14.001 (EHV), Technology Foundation Perspective Program 'Back2Roots' grant no. 14219 (PLT and CMJP), and ERC Advanced grant no. 269072 of the European Research Council (CMJP).

Author contributions

Conceptualization: PLT, EHV, and CMJP; Formal analysis: PLT, EHV, RRB, and KV; Funding acquisition: CMJP; Investigation: PLT, EHV, RRB, KV, and JAVP; Methodology: PLT, EHV, and JAVP; Supervision: PLT, EHV, and CMJP; Validation: PLT, EHV, RRB, and KV; writing of the manuscript: PLT, EHV, and CMJP.

Data availability

The data supporting the findings of this study are available from the corresponding author (Corné Pieterse) upon request.

References

Aznar A, Chen NW, Thomine S, Dellagi A. 2015*a*. Immunity to plant pathogens and iron homeostasis. Plant Science **240**, 90–97.

Aznar A, Patrit O, Berger A, Dellagi A. 2015*b*. Alterations of iron distribution in Arabidopsis tissues infected by *Dickeya dadantii*. Molecular Plant Pathology **16**, 521–528.

Bakker PAHM, Pieterse CMJ, de Jonge R, Berendsen RL. 2018. The soil-borne legacy. Cell **172**, 1178–1180.

Balk J, Schaedler TA. 2014. Iron cofactor assembly in plants. Annual Review of Plant Biology **65**, 125–153.

Ballini E, Nguyen TT, Morel JB. 2013. Diversity and genetics of nitrogen-induced susceptibility to the blast fungus in rice and wheat. Rice **6**, 32.

Beyer SF, Beesley A, Rohmann PFW, Schultheiss H, Conrath U, Langenbach CJG. 2019. The Arabidopsis non-host defence-associated

coumarin scopoletin protects soybean from Asian soybean rust. the Plant Journal **99**, 397–413.

Bloem E, Haneklaus S, Schnug E. 2015. Milestones in plant sulfur research on sulfur-induced-resistance (SIR) in Europe. Frontiers in Plant Science **5**, 779.

Broekgaarden C, Caarls L, Vos IA, Pieterse CM, Van Wees SC. 2015. Ethylene: traffic controller on hormonal crossroads to defense. Plant Physiology **169**, 2371–2379.

Brumbarova T, Bauer P, Ivanov R. 2015. Molecular mechanisms governing *Arabidopsis* iron uptake. Trends in Plant Science **20**, 124–133.

Colangelo EP, Guerinot ML. 2004. The essential basic helix–loop–helix protein FIT1 is required for the iron deficiency response. The Plant Cell **16**, 3400–3412.

Connorton JM, Balk J, Rodríguez-Celma J. 2017. Iron homeostasis in plants—a brief overview. Metallomics **9**, 813–823.

Czechowski T, Stitt M, Altmann T, Udvardi MK, Scheible WR. 2005. Genome-wide identification and testing of superior reference genes for transcript normalization in Arabidopsis. Plant Physiology **139**, 5–17.

Darbani B, Briat JF, Holm PB, Husted S, Noeparvar S, Borg S. 2013. Dissecting plant iron homeostasis under short and long-term iron fluctuations. Biotechnology Advances **31**, 1292–1307.

Dellagi A, Rigault M, Segond D, Roux C, Kraepiel Y, Cellier F, Briat JF, Gaymard F, Expert D. 2005. Siderophore-mediated upregulation of Arabidopsis ferritin expression in response to *Erwinia chrysanthemi* infection. The Plant Journal **43**, 262–272.

Durrant WE, Dong X. 2004. Systemic acquired resistance. Annual Review of Phytopathology **42**, 185–209.

Fenton H. 1894. Oxidation of tartaric acid in presence of iron. Journal of the Chemical Society, Transactions **65**, 899–910.

Fourcroy P, Sisó-Terraza P, Sudre D, Savirón M, Reyt G, Gaymard F, Abadía A, Abadia J, Alvarez-Fernández A, Briat JF. 2014. Involvement of the ABCG37 transporter in secretion of scopoletin and derivatives by *Arabidopsis* roots in response to iron deficiency. New Phytologist **201**, 155–167.

Fourcroy P, Tissot N, Gaymard F, Briat JF, Dubos C. 2016. Facilitated Fe nutrition by phenolic compounds excreted by the *Arabidopsis* ABCG37/PDR9 transporter requires the IRT1/FRO2 high-affinity root Fe^{2+} transport system. Molecular Plant **9**, 485–488.

García MJ, Corpas FJ, Lucena C, Alcántara E, Pérez-Vicente R, Zamarreño ÁM, Bacaicoa E, García-Mina JM, Bauer P, Romera FJ. 2018. A shoot Fe signaling pathway requiring the OPT3 transporter controls GSNO reductase and ethylene in *Arabidopsis thaliana* roots. Frontiers in Plant Science **9**, 1325.

Guerinot ML, Yi Y. 1994. Iron: nutritious, noxious, and not readily available. Plant Physiology **104**, 815–820.

Guzmán P, Ecker JR. 1990. Exploiting the triple response of *Arabidopsis* to identify ethylene-related mutants. The Plant Cell **2**, 513–523.

Hindt MN, Guerinot ML. 2012. Getting a sense for signals: regulation of the plant iron deficiency response. Biochimica et Biophysica Acta **1823**, 1521–1530.

Hirsch J, Marin E, Floriani M, Chiarenza S, Richaud P, Nussaume L, Thibaud MC. 2006. Phosphate deficiency promotes modification of iron distribution in *Arabidopsis* plants. Biochimie **88**, 1767–1771.

Howe GA, Jander G. 2008. Plant immunity to insect herbivores. Annual Review of Plant Biology **59**, 41–66.

Hsiao PY, Cheng CP, Koh KW, Chan MT. 2017. The *Arabidopsis* defensin gene, *AtPDF1*.1, mediates defence against *Pectobacterium carotovorum* subsp. *carotovorum* via an iron-withholding defence system. Scientific Reports **7**, 9175.

Khan GA, Vogiatzaki E, Glauser G, Poirier Y. 2016. Phosphate deficiency induces the jasmonate pathway and enhances resistance to insect herbivory. Plant Physiology **171**, 632–644.

Khan MA, Castro-Guerrero NA, McInturf SA, *et al.* 2018. Changes in iron availability in Arabidopsis are rapidly sensed in the leaf vasculature and impaired sensing leads to opposite transcriptional programs in leaves and roots. Plant, Cell & Environment **41**, 2263–2276.

Kieu NP, Aznar A, Segond D, Rigault M, Simond-Côte E, Kunz C, Soulie MC, Expert D, Dellagi A. 2012. Iron deficiency affects plant defence responses and confers resistance to *Dickeya dadantii* and *Botrytis cinerea*. Molecular Plant Pathology **13**, 816–827.

King EO, Ward MK, Raney DE. 1954. Two simple media for the demonstration of pyocyanin and fluorescin. Journal of Laboratory and Clinical Medicine **44**, 301–307.

Kobayashi T, Nozoye T, Nishizawa NK. 2019. Iron transport and its regulation in plants. Free Radical Biology & Medicine **133**, 11–20.

Koen E, Trapet P, Brulé D, *et al.* 2014. β-Aminobutyric acid (BABA)-induced resistance in *Arabidopsis thaliana*: link with iron homeostasis. Molecular Plant-Microbe Interactions **27**, 1226–1240.

Kunkel BN, Bent AF, Dahlbeck D, Innes RW, Staskawicz BJ. 1993. RPS2, an Arabidopsis disease resistance locus specifying recognition of *Pseudomonas syringae* strains expressing the avirulence gene avrRpt2. The Plant Cell **5**, 865–875.

Lapin D, Meyer RC, Takahashi H, Bechtold U, Van den Ackerveken G. 2012. Broad-spectrum resistance of Arabidopsis C24 to downy mildew is mediated by different combinations of isolate-specific loci. New Phytologist **196**, 1171–1181.

Leeman M, Den Ouden FM, Van Pelt JA, Dirkx FPM, Steijl H, Bakker PAHM, Schippers B. 1996. Iron availability affects induction of systemic resistance to fusarium wilt of radish by *Pseudomonas fluorescens*. Phytopathology **86**, 149–155.

Lucena C, Romera FJ, García MJ, Alcántara E, Pérez-Vicente R. 2015. Ethylene participates in the regulation of Fe deficiency responses in Strategy I plants and in rice. Frontiers in Plant Science **6**, 1056.

Luo B, Ma P, Nie Z, *et al.* 2019. Metabolite profiling and genome-wide association studies reveal response mechanisms of phosphorus deficiency in maize seedling. The Plant Journal **97**, 947–969.

Martinez-Medina A, Flors V, Heil M, Mauch-Mani B, Pieterse CMJ, Pozo MJ, Ton J, van Dam NM, Conrath U. 2016. Recognizing plant defense priming. Trends in Plant Science **21**, 818–822.

Martínez-Medina A, Van Wees SCM, Pieterse CMJ. 2017. Airborne signals from *Trichoderma* fungi stimulate iron uptake responses in roots resulting in priming of jasmonic acid-dependent defences in shoots of *Arabidopsis thaliana* and *Solanum lycopersicum*. Plant, Cell & Environment **40**, 2691–2705.

Mendoza-Cózatl DG, Xie Q, Akmakjian GZ, *et al.* 2014. OPT3 is a component of the iron-signaling network between leaves and roots and misregulation of *OPT3* leads to an over-accumulation of cadmium in seeds. Molecular Plant **7**, 1455–1469.

Nobori T, Velásquez AC, Wu J, Kvitko BH, Kremer JM, Wang Y, He SY, Tsuda K. 2018. Transcriptome landscape of a bacterial pathogen under plant immunity. Proceedings of the National Academy of Sciences, USA **115**, E3055–E3064.

Oñate-Sánchez L, Vicente-Carbajosa J. 2008. DNA-free RNA isolation protocols for *Arabidopsis thaliana*, including seeds and siliques. BMC Research Notes **1**, 93.

Pieterse CMJ, Berendsen RL, de Jonge R, Stringlis IA, Van Dijken AJH, Van Pelt JA, Van Wees SCM, Yu K, Zamioudis C, Bakker PAHM. 2020. *Pseudomonas simiae* WCS417: star track of a model beneficial rhizobacterium. Plant and Soil (in press).

Pieterse CM, Van der Does D, Zamioudis C, Leon-Reyes A, Van Wees SC. 2012. Hormonal modulation of plant immunity. Annual Review of Cell and Developmental Biology **28**, 489–521.

Pieterse CM, van Wees SC, Hoffland E, van Pelt JA, van Loon LC. 1996. Systemic resistance in Arabidopsis induced by biocontrol bacteria is independent of salicylic acid accumulation and pathogenesis-related gene expression. The Plant Cell **8**, 1225–1237.

Pieterse CM, van Wees SC, van Pelt JA, Knoester M, Laan R, Gerrits H, Weisbeek PJ, van Loon LC. 1998. A novel signaling pathway controlling induced systemic resistance in Arabidopsis. The Plant Cell **10**, 1571–1580.

Pieterse CM, Zamioudis C, Berendsen RL, Weller DM, Van Wees SC, Bakker PA. 2014. Induced systemic resistance by beneficial microbes. Annual Review of Phytopathology **52**, 347–375.

Robinson NJ, Procter CM, Connolly EL, Guerinot ML. 1999. A ferric-chelate reductase for iron uptake from soils. Nature **397**, 694–697.

Romera FJ, García MJ, Lucena C, Martínez-Medina A, Aparicio MA, Ramos J, Alcántara E, Angulo M, Pérez-Vicente R. 2019. Induced systemic resistance (ISR) and Fe deficiency responses in dicot plants. Frontiers in Plant Science **10**, 287.

Römheld V. 1987. Different strategies for iron acquisition in higher plants. Physiologica Plantarum **79**, 231–234.

Santi S, Schmidt W. 2009. Dissecting iron deficiency-induced proton extrusion in *Arabidopsis* roots. New Phytologist **183**, 1072–1084.

Schmid NB, Giehl RF, Döll S, Mock HP, Strehmel N, Scheel D, Kong X, Hider RC, von Wirén N. 2014. Feruloyl-CoA 6'-hydroxylase1-dependent coumarins mediate iron acquisition from alkaline substrates in Arabidopsis. Plant Physiology **164**, 160–172.

Schmittgen TD, Livak KJ. 2008. Analyzing real-time PCR data by the comparative C(T) method. Nature Protocols **3**, 1101–1108.

Segarra G, Elena G, Trillas I. 2013. Systemic resistance against *Botrytis cinerea* in Arabidopsis triggered by an olive marc compost substrate requires functional SA signalling. Physiological and Molecular Plant Pathology **82**, 46–50.

Segarra G, Van der Ent S, Trillas I, Pieterse CM. 2009. MYB72, a node of convergence in induced systemic resistance triggered by a fungal and a bacterial beneficial microbe. Plant biology **11**, 90–96.

Segond D, Dellagi A, Lanquar V, Rigault M, Patrit O, Thomine S, Expert D. 2009. *NRAMP* genes function in *Arabidopsis thaliana* resistance to *Erwinia chrysanthemi* infection. The Plant Journal **58**, 195–207.

Shen C, Yang Y, Liu K, Zhang L, Guo H, Sun T, Wang H. 2016. Involvement of endogenous salicylic acid in iron-deficiency responses in Arabidopsis. Journal of Experimental Botany **67**, 4179–4193.

Stacey MG, Patel A, McClain WE, Mathieu M, Remley M, Rogers EE, Gassmann W, Blevins DG, Stacey G. 2008. The Arabidopsis AtOPT3 protein functions in metal homeostasis and movement of iron to developing seeds. Plant Physiology **146**, 589–601.

Stassen MJJ, Hsu S-H, Pieterse CMJ, Stringlis IA. 2020. Coumarin communication along the microbiome–root–shoot axis. Trends in Plant Science doi:10.1016/j.tplants.2020.09.008.

Stringlis IA, de Jonge R, Pieterse CMJ. 2019. The age of coumarins in plant–microbe interactions. Plant & Cell Physiology **60**, 1405–1419.

Stringlis IA, Proietti S, Hickman R, Van Verk MC, Zamioudis C, Pieterse CMJ. 2018*a*. Root transcriptional dynamics induced by beneficial rhizobacteria and microbial immune elicitors reveal signatures of adaptation to mutualists. The Plant Journal **93**, 166–180.

Stringlis IA, Yu K, Feussner K, de Jonge R, Van Bentum S, Van Verk MC, Berendsen RL, Bakker PAHM, Feussner I, Pieterse CMJ. 2018*b*. MYB72-dependent coumarin exudation shapes root microbiome assembly to promote plant health. Proceedings of the National Academy of Sciences, USA **115**, E5213–E5222.

Thalineau E, Fournier C, Gravot A, Wendehenne D, Jeandroz S, Truong HN. 2018. Nitrogen modulation of *Medicago truncatula* resistance to *Aphanomyces euteiches* depends on plant genotype. Molecular Plant Pathology **19**, 664–676.

Thalineau E, Truong HN, Berger A, Fournier C, Boscari A, Wendehenne D, Jeandroz S. 2016. Cross-regulation between N metabolism and nitric oxide (NO) signaling during plant immunity. Frontiers in Plant Science **7**, 472.

Thomma BP, Eggermont K, Tierens KF, Broekaert WF. 1999. Requirement of functional *ethylene-insensitive* 2 gene for efficient resistance of Arabidopsis to infection by *Botrytis cinerea*. Plant Physiology **121**, 1093–1102.

Ton J, Davison S, Van Wees SC, Van Loon L, Pieterse CM. 2001. The arabidopsis *ISR1* locus controlling rhizobacteria-mediated induced systemic resistance is involved in ethylene signaling. Plant Physiology **125**, 652–661.

Ton J, Jakab G, Toquin V, Flors V, Iavicoli A, Maeder MN, Métraux JP, Mauch-Mani B. 2005. Dissecting the beta-aminobutyric acid-induced priming phenomenon in Arabidopsis. The Plant Cell **17**, 987–999.

Trapet P, Avoscan L, Klinguer A, Pateyron S, Citerne S, Chervin C, Mazurier S, Lemanceau P, Wendehenne D, Besson-Bard A. 2016. The *Pseudomonas fluorescens* siderophore pyoverdine weakens *Arabidopsis thaliana* defense in favor of growth in iron-deficient conditions. Plant Physiology **171**, 675–693.

Tsai HH, Schmidt W. 2017. Mobilization of iron by plant-borne coumarins. Trends in Plant Science **22**, 538–548.

van Damme M, Zeilmaker T, Elberse J, Andel A, de Sain-van der Velden M, van den Ackerveken G. 2009. Downy mildew resistance in Arabidopsis by mutation of *HOMOSERINE KINASE*. The Plant Cell **21**, 2179–2189.

Van der Ent S, Verhagen BW, Van Doorn R, *et al.* 2008. *MYB72* is required in early signaling steps of rhizobacteria-induced systemic resistance in Arabidopsis. Plant Physiology **146**, 1293–1304.

Van Kan JAL, Stassen JHM, Mosbach A, *et al.* 2017. A gapless genome sequence of the fungus *Botrytis cinerea*. Molecular Plant Pathology **18**, 75–89.

Van Wees SC, Van Pelt JA, Bakker PA, Pieterse CM. 2013. Bioassays for assessing jasmonate-dependent defenses triggered by pathogens, herbivorous insects, or beneficial rhizobacteria. Methods in Molecular Biology **1011**, 35–49.

Verbon EH, Trapet PL, Kruijs S, Temple-Boyer-Dury C, Rouwenhorst TG, Pieterse CMJ. 2019. Rhizobacteria-mediated activation of the Fe deficiency response in Arabidopsis roots: impact on Fe status and signaling. Frontiers in Plant Science **10**, 909.

Verbon EH, Trapet PL, Stringlis IA, Kruijs S, Bakker PAHM, Pieterse CMJ. 2017. Iron and immunity. Annual Review of Phytopathology **55**, 355–375.

Vert G, Grotz N, Dédaldéchamp F, Gaymard F, Guerinot ML, Briat JF, Curie C. 2002. IRT1, an Arabidopsis transporter essential for iron uptake from the soil and for plant growth. The Plant Cell **14**, 1223–1233.

Vlot AC, Klessig DF, Park SW. 2008. Systemic acquired resistance: the elusive signal(s). Current Opinion in Plant Biology **11**, 436–442.

Wildermuth MC, Dewdney J, Wu G, Ausubel FM. 2001. Isochorismate synthase is required to synthesize salicylic acid for plant defence. Nature **414**, 562–565.

Wu J, Baldwin IT. 2010. New insights into plant responses to the attack from insect herbivores. Annual Review of Genetics **44**, 1–24.

Yi Y, Guerinot ML. 1996. Genetic evidence that induction of root Fe(III) chelate reductase activity is necessary for iron uptake under iron deficiency. The Plant Journal **10**, 835–844.

Zamioudis C, Hanson J, Pieterse CM. 2014. β-Glucosidase BGLU42 is a MYB72-dependent key regulator of rhizobacteria-induced systemic resistance and modulates iron deficiency responses in Arabidopsis roots. New Phytologist **204**, 368–379.

Zamioudis C, Korteland J, Van Pelt JA, *et al.* 2015. Rhizobacterial volatiles and photosynthesis-related signals coordinate *MYB72* expression in Arabidopsis roots during onset of induced systemic resistance and iron-deficiency responses. The Plant Journal **84**, 309–322.

Zhai Z, Gayomba SR, Jung HI, *et al.* 2014. OPT3 is a phloem-specific iron transporter that is essential for systemic iron signaling and redistribution of iron and cadmium in Arabidopsis. The Plant Cell **26**, 2249–2264.

Zhang Y, Li X. 2019. Salicylic acid: biosynthesis, perception, and contributions to plant immunity. Current Opinion in Plant Biology **50**, 29–36.